The Use of Kirchhoff's Method in Jet Aeroacoustics

Final Report
NASA/NAG 1-~~1686~~ 1605 (3/1/94-9/15/94)

Principal Investigator: Anastasios S. Lyrintzis
Associate Professor
School of Aeronautics and Astronautics
Purdue University
W. Lafayette, IN 47907-1282

Participant: Anthony Pilon
Aerospace Engineering & Mechanics
University of Minnesota
Minneapolis, MN 55455

Technical Monitor: Kristine Meadows (MS 128)
NASA Langley Research Center,
Hampton, VA 23665

Abstract

Supersonic jet aeroacoustics will be studied using computational techniques. In the study, a Kirchhoff method is used to predict flow generated noise in the mid– and far–fields. This type of method shows promise because it is based on surface integrals and not the volume integrals found in traditional acoustic prediction methods. The Kirchhoff method is dependent on accurate prediction of flow variables in the near–field. Here, computational fluid dynamics (CFD) programs are used for these predictions. Specifically, an existing large eddy simulation (LES) code will be modified for aeroacoustic applications. Issues involved in the implementation of the Kirchhoff method as well as the coupling with the CFD code will be discussed. Important physical noise parameters will be identified and investigated in the study.

1. Introduction

The noise generated by supersonic jets is a major concern in the development of future aircraft. Aerodynamically generated noise has been found to be a major contributor to jet noise.[1] Accurate prediction and reduction of this flow generated noise is essential.

This project is aimed at predicting the noise of supersonic jets with a new approach. This method is based on the electro-magnetic theory presented by Kirchhoff in 1882.[2] In this approach, the Kirchhoff method, mid- and far-field sound is predicted from flow quantities on an arbitrary surface. For this prediction, a linear wave equation is assumed to be valid outside the surface. Thus, the surface must enclose all linear and non-linear sources of sound, and any reflecting physical surfaces. The needed quantities on the Kirchhoff surface can be determined in several different ways. Theoretical expressions, experimental data, or computational fluid dynamics (CFD) methods can all be employed. For this study, the combined CFD–Kirchhoff method is used. This requires judicious placement of the Kirchhoff surface as well as a spatially and temporally accurate CFD code. These issues are discussed further herein.

2. Jet Noise

As mentioned previously, aerodynamically generated noise is a major concern in the development of future aircraft. A summary of subsonic and supersonic jet noise is given in this section.

The earliest comprehensive work on sound generated by fluid motion was presented by Lighthill.[3] Lighthill noted that the total energy radiated outward as sound from an unsteady flow is a small fraction of the flow's total kinetic energy. Approximating this radiation may lead to an incorrect solution. Lighthill introduced his *acoustic analogy* to overcome this difficulty. In the acoustic analogy, the entire unsteady flow field is replaced by an equivalent volume distribution of acoustic sources. The sources may move, but the surrounding fluid medium cannot. All unsteady fluid dynamics are included in the strength and distribution of acoustic sources. Lighthill's equation can be derived by subtracting the the divergence of the momentum equation from the time derivative of the continuity equation. The resulting inhomogeneous wave equation is

$$\frac{\partial^2 \rho}{\partial t^2} - a^2 \nabla^2 \rho = \frac{\partial^2 T_{i,j}}{\partial x_i \partial x_j} \tag{2.1}$$

where $T_{i,j}$ is the Lighthill stress tensor

$$T_{i,j} = \rho u_i u_j + \left(p - \rho a^2\right) \delta_{i,j} - \tau_{i,j} \tag{2.2}$$

Here u_i are the cartesian velocity components, ρ is the density, p is the pressure, a the ambient speed of sound, and $\tau_{i,j}$ is the viscous stress tensor. If the entire unsteady flow field is approximated with acoustic sources, Lighthill's equation is exact, and has the following solution for an unbounded flow

$$\rho(\vec{x}, t) = \frac{1}{4\pi a^2} \int_V \left[\frac{1}{|\vec{x} - \vec{y}|} \frac{\partial^2 T_{i,j}}{\partial x_i \partial x_j} \right] dy \tag{2.3}$$

where $\vec{y}$ is the source location, and $\vec{x}$ is the observer location. The brackets indicate evaluation at the retarded time,

$$\tau = t - \frac{|\vec{x} - \vec{y}|}{a} \tag{2.4}$$

Several observations can be made from the solution to Lighthill's equation. First, the double divergence of the stress tensor indicates quadrupole type radiation. This agrees with the assumption that acoustically radiated energy is a small fraction of the flow kinetic energy. Also, since quadrupoles are highly directional, the emitted sound will have a great deal of directivity. It is also important to note that the solution to Lighthill's equation requires a volume integral, and that the entire unsteady flow field must be known to calculate the acoustic sources. This is possible theoretically in cases of academic interest, or if the field is determined experimentally or computationally. It is possible, however, to make order of magnitude approximations to the terms in Lighthill's equation. In doing this it can be shown that for cold, subsonic jets, the acoustic intensity scales with the eighth power of the jet velocity.[3] It is important to note here that, in his analysis, Lighthill omitted the effects of density variations within the jet on sound generation. These variations become important if the jet is heated, or if the Mach number approaches or exceeds 1.[4]

In the shear layer of a jet most turbulence dynamics statistics change very slowly in the downstream direction. This implies that locally the flow is in dynamic equilibrium. Statistical mechanics then says that the large scale turbulent fluctuations (vortical structures) can be represented by a superposition of normal modes of the system. For jet flows the normal modes are the instability waves which are calculated with the compressible Rayleigh or Orr–Sommerfeld equations. Thus, it is meaningful in a statistical sense to represent the large scale vortical structures as a superposition of instability waves.[1] Experiments have shown that the noise generated by jets is due primarily to these large scale structures. Instability wave solutions have also been used as source predictions in the acoustic analogy method.[5,6] Tam and others have also used matched asymptotic expansions with instability wave solutions to extend the generated sound to the far–field.

Since the large scale turbulent structures are the dominant source of noise, the fine grain turbulence can be modeled. The sound generated by the large turbulence structures is then calculated directly. This approach was utilized by Mankbadi, et al.[7] This method will also be used in the current study, and is discussed further herein.

If a supersonic jet is not perfectly expanded (operating at off–design conditions) a shock cell structure will develop. It is possible for the large scale structures to interact with the shocks in such a way as to set up an acoustic feedback system. This feedback system allows the production of very high intensity sound to be propagated to the far field. This "screech" phenomena is not yet well understood, and will be extensively investigated in the current study.

It is relevant to discuss here the different characteristics of supersonic jet noise. The first relevant characteristic is turbulent mixing noise. Turbulent mixing noise is due to the mixing and interaction of large turbulent structures that occurs near the shear layer of the jet. This noise is located at the low frequency end of the power spectrum. If the jet is imperfectly expanded there may also be screech tones, as discussed above. The screech tones are discrete frequency spikes in the power spectrum, located at the feedback

frequency, and possibly some harmonics. The screech tones are the lower bound for the broadband shock associated noise. The broadband shock noise is due to the motion of shocks and their interaction with turbulence. Higher frequencies are mainly due to fine scales of turbulence.

3. Computational Aeroacoustics Methods

Several different methods are currently being used for computational aeroacoustic predictions. A few of the more popular methods are described below.

1. *Lighthill's Acoustic Analogy.* In the acoustic analogy[3] approach to aeroacoustics, equation (2.3), or a similar equation, is solved numerically. The far–field pressure is then calculated in a volume integral over the domain containing the sound sources. Several researchers, most notably Lilly[5] and Ffowcs Williams and Hawkings,[8] have proposed modifications to Lighthill's original formula to account for the effects of sound–flow interaction, and surfaces in the source domain.

The main difficulty involved in the acoustic analogy approach is the evaluation of the quadrupole terms and the volume integral. If the source region is not compact, retention of terms in time and space will lead to storage problems.

2. *Full Flow–Field CFD.* This method involves using a CFD method to calculate pressure disturbances into the far–field. Since traditional CFD schemes tend to have dissipation and dispersion properties that damp out acoustic oscillations, different methods are applied here. These methods have high orders of accuracy, and often employ grid refinement strategies. Recent full CFD methods include the Dispersion Relation Preserving (DRP) scheme of Tam and Webb,[9] and an upwind version of the leapfrog scheme due to Thomas and Roe.[10]

A major problem involved in this type of method is the need for a very fine grid to resolve the acoustic fluctuations. Use of a fine grid in the mid– and far–fields will lead to storage problems. Also, since the acoustic fluctuations are quite small, the use of non–linear equations (Euler or Navier–Stokes) can result in errors.[11]

3. *CFD with Linearized Euler Equations.* In this method, a nonlinear near–field CFD solution is coupled with a far–field solution determined from the linearized Euler equations. This method requires the use of proper boundary conditions between the near– and far–fields. In addition, far–field mesh spacing, diffusion, and dispersion errors must be addressed. However, this method seems to have potential, due to the reduced storage requirements as compared to a full CFD approach, or the acoustic analogy. Mankbadi, et al[12] have used this approach to determine the far–field sound due to a perfectly expanded supersonic jet.

4. *CFD–Kirchhoff Approach.* This method (the Kirchhoff method) utilizes CFD techniques to determine the nonlinear near–field. The far–field is determined from a linear Kirchhoff formulation. The Kirchhoff formulation is defined on a control surface which must enclose all sound sources. The full nonlinear flow equations are solved in the near– and mid–fields through the use of a CFD application. A surface integral of the solution variables over the control surface gives enough information to determine the sound at any point in the far–field. This method provides for adequate matching between the aerodynamic nonlinear near–field and the acoustic linear far–field.

One major advantage of this method is the need for only surface integrals. This greatly reduces storage requirements. The method accounts for full diffraction and focusing effects, as well as non-compactness. Additionally, nonlinear shock effects can be easily accounted for. The Kirchhoff method has been used extensively for prediction of helicopter and turbomachinery noise.[13] A review of the various uses of the Kirchhoff method in aeroacoustics was presented by Lyrintzis.[14] In this study, the author will use the Kirchhoff method to investigate the aeroacoustics of supersonic jets. Since the method can handle shock associated noise, excellent results are expected for imperfectly expanded jets.

4. Derivation of the Kirchhoff Method

The time domain formulation of the Kirchhoff method is derived in this section. A simple transformation is then used to create the frequency domain formulation. Additionally, the application of the Kirchhoff method to supersonic jet aeroacoustics will be discussed. For the sake of brevity, only the particular Kirchhoff formulations to be used in the study will be derived.

To derive the Kirchhoff method for supersonic jet aeroacoustics, it is first assumed that there is a (rigid) control surface S which encloses all aerodynamic nonlinearities and sound sources in the flow field. A further assumption is made in that the free stream is moving at a steady, subsonic velocity. Thus the surface S moves with this velocity, U_∞. Outside S, the pressure perturbations are governed by a convective wave equation

$$\nabla^2 p - \frac{1}{a^2}\left(\frac{\partial}{\partial t} + U_\infty \frac{\partial}{\partial x}\right)^2 p = 0 \tag{4.1}$$

where p is the pressure, and a is the ambient speed of sound. This equation is solved in the far field through the use of a Green's function approach for hyperbolic equations. After some algebra,[15] the pressure field can be expressed using surface integrals

$$p(\vec{x},t) = -\frac{1}{4\pi}\int_{S_0}\left[\frac{p}{r_0^2}\frac{\partial r_0}{\partial n_0} + \frac{1}{r_0}\frac{\partial p}{\partial n_0} + \frac{1}{a r_0 \beta^2}\frac{\partial p}{\partial t}\left(\frac{\partial r_0}{\partial n_0} - M_\infty \frac{\partial x_0}{\partial n_0}\right)\right]_\tau dS_0 \tag{4.2}$$

where r_0 is the distance between the observer and the source in Prandtl-Glauert coordinates

$$r_0 = \left[(x-x_s)^2 + \beta^2 (y-y_s)^2 + \beta^2 (z-z_s)^2\right]^{\frac{1}{2}} \tag{4.3}$$

The retarded time, τ and time delay, t_d are given by

$$\tau = t - t_d = t - \frac{[r_0 - M_\infty (x-x_s)]}{a\beta^2} \tag{4.4}$$

(Subscript $_0$ denotes Prandtl-Glauert transformed variables, $(x_0, y_0, z_0) = (x, \beta y, \beta z)$, and $\beta = \sqrt{1-M_\infty^2}$.) Here, $\vec{n}$ is the unit outward normal to the surface S, and subscript τ denotes evaluation at the retarded time.

With equation (4.2) it is possible to calculate the acoustic signature at any point outside of S from the pressure and it's normal and time derivatives on the surface. These

quantities can be determined from theory, experiment, or computational methods. In this study, a temporally and spatially accurate CFD code is used to determine the quantities. The CFD codes utilized will be discussed in a later section.

Researchers in aeroacoustics are often concerned with dominant frequencies. That is, they are interested with how a sound source varies with frequency as much as with time. For this reason, a Fourier transform is often performed to obtain a power spectrum. A recent development with the Kirchhoff method allows the researcher to work directly in the frequency domain. This derivation is due to Lyrintzis,[14] although a similar expression was derived by Davis and Atassi.[16]

The derivation of the frequency domain Kirchhoff method is straightforward. In this approach, the derivation begins with the Helmholtz equation, and the pressure is written as

$$p(\vec{x},t) = \Re\left\{\hat{p}(\vec{x})\, e^{-i\omega t}\right\} \tag{4.5}$$

This expression is then substituted into equation (4.2) to obtain

$$p(\vec{x},t) = \Re\left\{ -\frac{e^{i\omega t}}{4\pi}\int_{S_0}\left[\frac{\hat{p}}{r_0^2}\frac{\partial r_0}{\partial n_0} + \frac{1}{r_0}\frac{\partial \hat{p}}{\partial n_0} - \frac{i\omega}{a r_0 \beta^2}\hat{p}\left(\frac{\partial r_0}{\partial n_0} - M_\infty \frac{\partial x_0}{\partial n_0}\right)\right]\cdot \right.$$
$$\left. \exp\left(i\frac{\omega}{a\beta^2}\left(r_0 + M_\infty (x_s - x)\right)\right) dS_0 \right\}. \tag{4.6}$$

This formulation allows the user to perform a Fourier transform on the initial CFD data before using the Kirchhoff method instead of after it's use. There may be advantages to this sequence, in that there may be a smaller phase error associated with working in the frequency domain.

To apply the Kirchhoff method to supersonic jet aeroacoustics the surface S is chosen as a cylinder surrounding the flow. Proper placement of this cylinder is essential for accurate predictions. The surface must enclose all nonlinearities in the flow. But, if it is placed too far away from the shear layer, grid stretching in the CFD program will lead to errors in the derivatives. Additionally, it may be difficult, or impossible, to enclose all nonlinearities in the axial direction. That is, the cylinder end surface might cut off noise producing portions of the flow. The cylinder end can be moved far downstream to ensure capturing of all nonlinearities, but then grid stretching and storage problems can occur. It may also be possible to use the Kirchhoff method with an incompletely closed surface, i.e. a cylinder with no end surface. Amplitude and phase errors caused by this omission have been calculated for simple acoustic source flows and will be discussed in a later section.

5. CFD Codes

The CFD methods used to calculate the near-field flow properties for the Kirchhoff method must have a high order of accuracy in both space and time in order to resolve the small amplitude acoustic fluctuations. A turbulence model is also necessary to include the effects that small scale turbulence has on the noise generation mechanisms. In this

section, proposed modifications to an existing CAA (computational aeroacoustics) code will be discussed.

As mentioned in a previous section, the large scale vortical structures account for most of the noise generation in supersonic jets. Because of this, it may be effective to resolve these large scales directly in the CFD calculations, and to model the smaller scale turbulence. This type of modeling is effectively accomplished with a large eddy simulation (LES) method. In LES methods eddies or vortical structures smaller than a filter width (grid cell size) are modeled using an eddy viscosity. One computational method that employs this scheme in solving the Navier–Stokes equations has been utilized by Mankbadi et. al.[7] This method, and some proposed modifications, are outlined below.

The computational method in consideration is referred to as a 2-4 MacCormack method, indicating second order accuracy in time, and fourth order accuracy in space. Currently, it is used to solve the filtered, axisymmetric Navier–Stokes equations

$$\frac{\partial U}{\partial t} + \frac{\partial F}{\partial x} + \frac{1}{r}\frac{\partial (rG)}{\partial r} = W \tag{5.1}$$

where U is the vector of unknowns and W is the source vector,

$$U = \begin{pmatrix} \overline{\rho} \\ \overline{\rho}\tilde{u} \\ \overline{\rho}\tilde{v} \\ \overline{\rho}\tilde{e} \end{pmatrix} \qquad W = \frac{1}{r}\begin{pmatrix} 0 \\ 0 \\ \overline{p} - \overline{\tau}_{\theta\theta} \\ 0 \end{pmatrix}$$

F and G are the fluxes in the axial and radial directions

$$F = \begin{pmatrix} \overline{\rho}\tilde{u} \\ \overline{\rho}\tilde{u}^2 + \overline{p} - \tau_{xx} \\ \overline{\rho}\tilde{u}\tilde{v} - \tau_{xr} \\ (\overline{\rho}\tilde{e} + \overline{p})\,\tilde{u} - \tilde{u}\tau_{xx} - \tilde{v}\tau_{xr} - kT_x \end{pmatrix} \qquad G = \begin{pmatrix} \overline{\rho}\tilde{v} \\ \overline{\rho}\tilde{u}\tilde{v} - \tau_{xr} \\ \overline{\rho}\tilde{v}^2 + \overline{p} - \tau_{rr} \\ (\overline{\rho}\tilde{e} + \overline{p})\,\tilde{v} - \tilde{u}\tau_{xr} - \tilde{v}\tau_{rr} - kT_r \end{pmatrix}$$

An overbar denotes a filtered quantity, and a tilde denotes Favre averaging.

$$\tilde{f} = \frac{\overline{\rho f}}{\overline{\rho}}$$

and $\tau_{i,j}$ are the viscous shear stresses. The stresses are split as $\tau = \overline{\tau}_v + \tau_t$ where subscript v denotes the viscous part and subscript t denotes the turbulent portion that needs to be modeled.

When performing an LES computation the governing equations are filtered for a certain length scale, resulting in residual turbulent stresses. Currently, Smagorinski's[17] model is used to resolve these stresses.

$$\tau_{t\,i,j} = \frac{1}{3}q_R^2\delta_{i,j} - 2\rho\nu_R R_{i,j} \tag{5.2}$$

where q_R is the energy of the residual turbulence. This term is incorporated into the thermodynamic pressure term and can be neglected. $R_{i,j}$ is the strain rate of the resolved scales.

$$R_{i,j} = \frac{1}{2}\left(\frac{\partial \tilde{u}_i}{\partial x_j} + \frac{\partial \tilde{u}_j}{\partial x_i}\right) \tag{5.3}$$

and ν_R is the effective viscosity of the residual field. Currently, the following definition is used for ν_R

$$\nu_R = (C_s\Delta)^2 \left(2R_{m,n}R_{m,n}\right)^{\frac{1}{2}} \tag{5.4}$$

where Δ is the filter width, $\Delta = (\Delta x \cdot \Delta r)^{\frac{1}{2}}$ and C_s is 0.23. It is possible that Smagorinski's model may not be the most appropriate for the aeroacoustic applications discussed here. If possible, a better model will be determined, or C_s may be determined dynamically based on flow variables.

As mentioned earlier, 2-4 accuracy is maintained in the code. This accuracy is achieved through an operator splitting, i.e.

$$U^{n+2} = L_x L_r L_r L_x U^n \tag{5.5}$$

where L_x and L_r are the one dimensional differential operators in the x and r directions. Superscripts n and $n+2$ refer to the current time level and the solution after temporal advancement. The full differential operators are listed in the appendix.

The LES method defined above works well for the calculation of perfectly expanded jets, and has been used in conjunction with a Kirchhoff method to predict far field sound.[18] But, due to the nature of the discretizations, it cannot calculate jet flows which contain shock waves. Thus, in order to predict imperfectly expanded jet flows, the differential operators need to be modified. The operators must be modified in such a way as to capture the shock waves while maintaining high order spatial and temporal accuracy. Additionally, the code should be extended to handle full three dimensional flows so that predictions can be performed on the 3D directivity inherent in supersonic jets (e.g. helical and flapping modes). The proposed modifications are outlined below.

Several types of high order shock capturing computational methods have been developed recently.[19] These include the total variation diminishing (TVD) and essentially non–oscillatory (ENO) schemes. While TVD schemes capture shock waves effectively, they necessarily degenerate to first order accuracy in doing so. This leaves TVD schemes unacceptable for aeroacoustics applications. ENO methods[20] use an adaptive, nonlinear computational stencil to avoid this problem. In this study, the ENO scheme of Atkins[21] will be applied to the conservation equations outlined above, while maintaining the LES turbulence modeling. Temporal accuracy will be maintained, or increased, through the use of the TVD–Runge–Kutta schemes of Shu.[22] A brief description of the ENO modifications follows.

In the ENO method, the goal is to approximate $\frac{\partial F}{\partial x}$ or $\frac{\partial G}{\partial y}$ to high order of accuracy, even in the presence of discontinuities. An approximation to $\frac{\partial F}{\partial x}$ that is said to be N^{th} order accurate is

$$\frac{\partial F}{\partial x}(x_i) = \frac{\overline{F}\left(x_{i+\frac{1}{2}}\right) - \overline{F}\left(x_{i-\frac{1}{2}}\right)}{\Delta x} + \mathcal{O}\left(\Delta x^N\right) \tag{5.6}$$

(An overbar now denotes a numerical approximation.) $\overline{F}$ can be defined generically in terms of F and it's derivatives by a Taylor series expansion

$$\overline{F}(x) = \sum_{n=0}^{N} a_n \Delta x^n \frac{\partial^n F(x)}{\partial x^n} \tag{5.7}$$

If (5.6) is enforced, and $\overline{F}(F(w), \ldots F(w), \ldots F(w)) = F(w)$ then the coefficients a_n of (5.7) can be uniquely determined. A further approximation can now be made in that $F(x_i)$ is approximated by a M^{th} order polynomial, $\Psi_i^M(x, F)$ through $M+1$ points in the neighborhood of i. Thus,

$$\overline{F}_i(x) = \sum_{n=0}^{N} a_n \Delta x^n \frac{\partial^n \Psi^M(x, F)}{\partial x^n} \tag{5.8}$$

which, when differenced, approximates the derivative via

$$\frac{\partial F}{\partial x}(x_i) = \frac{\overline{F}_i\left(x_{i+\frac{1}{2}}\right) - \overline{F}_i\left(x_{i-\frac{1}{2}}\right)}{\Delta x} + \mathcal{O}\left(\Delta x^N, \Delta x^M\right) \tag{5.9}$$

To eliminate the Gibb's phenomena found with most high order methods, Ψ_i^M is not necessarily centered on point i. A search algorithm is used to determine the $M+1$ "smoothest" points in the neighborhood of i. Ψ then gives a smooth approximation to F, and thus $\frac{\partial F}{\partial x}$ can be approximated without spurious oscillations, even at the discontinuity.

The ENO method described above has been evaluated for aeroacoustic applications (without LES modeling) by Casper and Meadows[23] with favorable results. They used high order accurate boundary conditions due to Atkins and Casper.[24] Using these boundary conditions may help improve the predictions in the current study as well.

6. Preliminary Results

Several factors must be evaluated before the CFD–Kirchhoff method can be utilized in the study of jet aeroacoustics. Lyrintzis and Mankbadi[18] investigated the effect of CFD grid (spatial) and temporal discretizations on the accuracy of the method. They found that it is relatively easy to obtain a suitable number of spatial points per acoustic wavelength or temporal points per acoustic period with existing CFD codes.

It is necessary to show that the Kirchhoff method can indeed accurately calculate an acoustic field. To this end, the Kirchhoff method has been used to calculate the acoustic fields, at an instant in time, produced by simple acoustic sources. Since the simple sources have analytical solutions, a direct comparison can be made.

Figure 1a shows the pressure contours for a point acoustic source (monopole) in a stagnant medium. Figure 1b shows the same field, except that there is a uniform velocity of Mach number 0.5 in the x direction. The analytical expression for pressure due to an acoustic source with unit amplitude is

$$p_s(\vec{x}) = \frac{1}{r_0} \sin\left[\omega\left(t - \frac{r_0 + M_\infty(x_s - x)}{a\beta^2}\right)\right] \tag{6.1}$$

where $\vec{r} = (x, y, z)$ is the observer location, and $\vec{r}_s = (x_s, y_s, z_s)$ is the source location. Subscript $_0$ denotes transformation to the Prandtl-Glauert coordinates, as before.

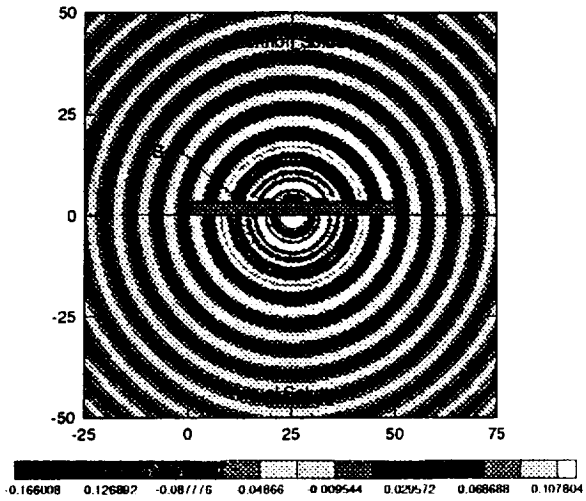

Figure 1a. Pressure contours for a point acoustic source. $M_\infty = 0.0$

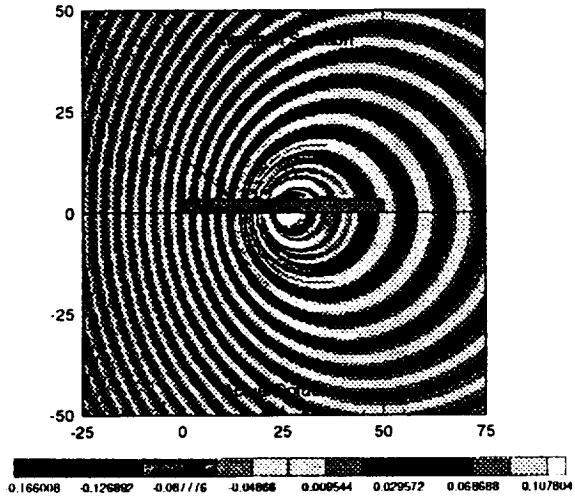

Figure 1b. Pressure contours for a point acoustic source. $M_\infty = 0.5$

In figures 1 the acoustic source is placed at $(25, 0, 0)$. The upper half of the figures shows the solution obtained with the Kirchhoff method, while the lower half shows the analytical solution obtained from (6.1). The cylindrical control surface, S, is labeled. The contours from the Kirchhoff and analytical solutions are nearly identical on both plots. One exception is the interior of the Kirchhoff surface, where the amplitude should be identically zero. The plots show an acceptable, small amplitude in this area.

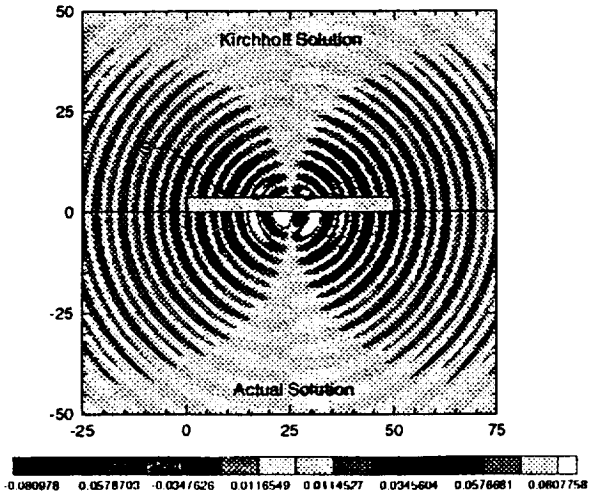

Figure 2a. Pressure contours for a point acoustic dipole. $\Theta_d = 0^o, M_\infty = 0.0$

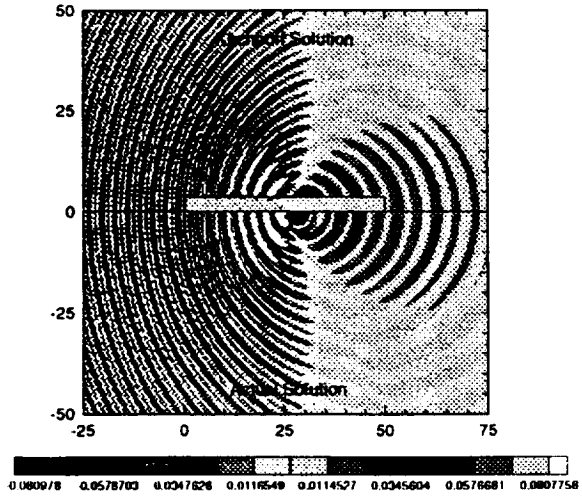

Figure 2b. Pressure contours for a point acoustic dipole. $\Theta_d = 0^o, M_\infty = 0.5$

Since there is a great deal of directivity in supersonic jets, it is also useful to use the

is the divergence of monopole radiation, i.e.

$$p_d(\vec{x}) = \nabla \cdot p_s(\vec{x})\,\hat{k} \tag{6.2}$$

where $\hat{k}$ is the unit vector which points along the axis of the dipole. Thus, there is maximum radiation in the direction of $\hat{k}$, and no radiation normal to $\hat{k}$ (for a stagnant free stream). For the radiation in figures 2, $\hat{k}$ is chosen to be $(1,0,0)$ to maintain symmetry about the x axis. From the figures it can be seen that the Kirchhoff method reproduces the contours quite well, including the inherent directivity. The pressure amplitude within the Kirchhoff surface is again nearly zero.

It may be difficult to enclose all nonlinear noise producing portions of the flow field when calculating the acoustic signatures of jets. That is, the nonlinear region may extend many jet diameters downstream of the jet orifice. Enclosing this entire 3D flow field can lead to storage problems. It may, however, be sufficient to use the Kirchhoff method on a portion of the flow field instead. If this is the case, the cylinder ends of the Kirchhoff surface are ignored. Ignoring these portions of the control surface will lead to errors in the amplitude and phase of the observed far–field acoustic signature, but they may be small enough to allow for an acceptable prediction.

Calculations of simple acoustic sources were again used to determine if the ends of the control surface can be ignored. Figures 3 show contours of the percentage amplitude and phase errors in the region downstream of a cylindrical control surface of length 50 and radius 4. For these calculations, a point acoustic source was placed at $(25,0)$. The percentage RMS amplitude error was calculated with

$$E_A = 100\frac{\mathrm{RMS}(p_{kir}) - \mathrm{RMS}(p_{act})}{\mathrm{RMS}(p_{act})}$$

while the percentage phase error was calculated with

$$E_P = 100\frac{(t_{kir} - t_{act})}{T}$$

where T is the period of the oscillations.

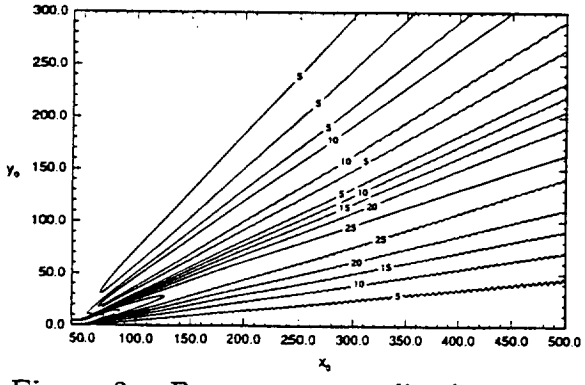

Figure 3a. Percentage amplitude error contours for a point acoustic source. $M_\infty = 0.0$

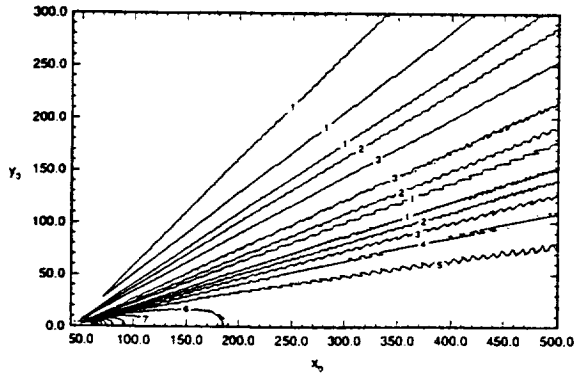

Figure 3b. Percentage phase error contours for a point acoustic source. $M_\infty = 0.0$

Figures 3 show that there is 5 to 30 percent error in amplitude in an area between 10^o and 45^o from the end of the cylinder. The highest amplitude error is in the region around $\Theta = 30^o$, where Θ is the angle measured from the positive x axis. The phase error is between one and ten percent (except near the cylinder base), and is in the same region as the amplitude error. The peak phase error occurs near the x axis. Similar error plots were obtained for radiation from dipoles of various orientations.

It would be desirable to determine a region where the Kirchhoff solution would be acceptable, even without the complete control surface. The errors in figures 3 are still too high to give an acceptable acoustic prediction. Thus, it is necessary to continue the calculations into the far-field to determine if the errors fall below acceptable levels.

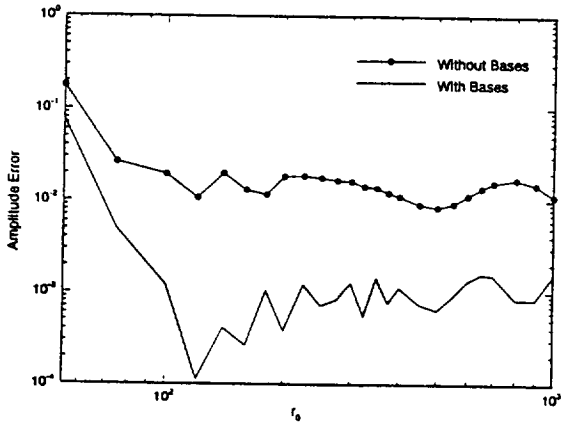

Figure 4a. Amplitude Error with distance at $\Theta = 0^o$. Point acoustic source.

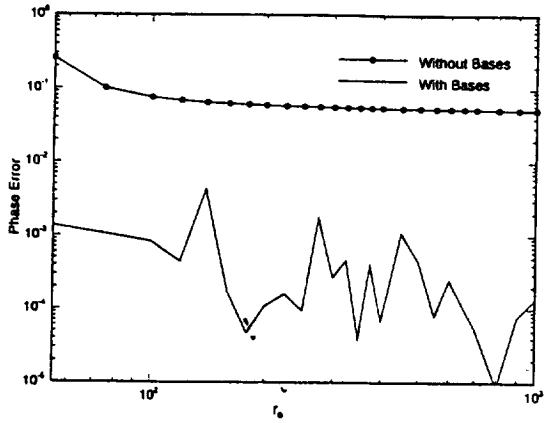

Figure 4b. Phase Error with distance at $\Theta = 0^o$. Point acoustic source.

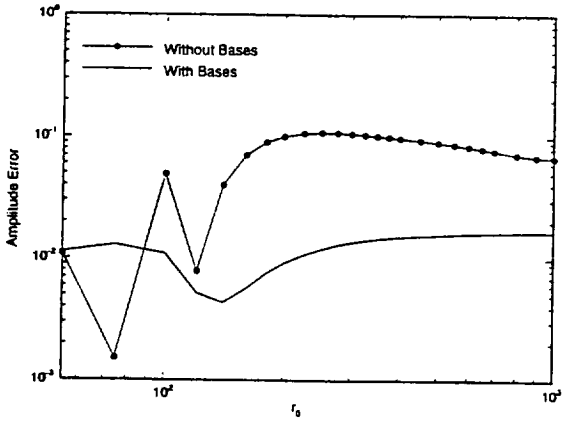

Figure 4c. Amplitude Error with distance at $\Theta = 30^o$. $\Phi_d = 30^o$ acoustic dipole.

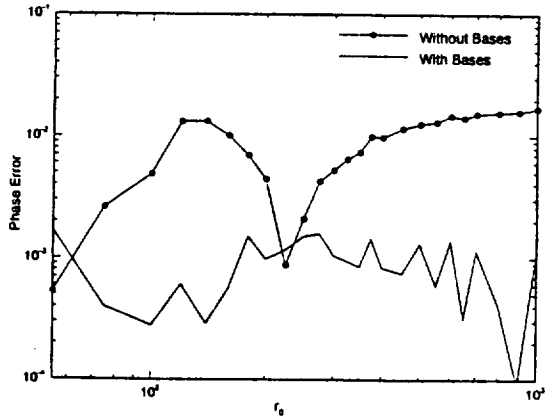

Figure 4d. Phase Error with distance at $\Theta = 30^o$. $\Phi_d = 30^o$ acoustic dipole.

The calculations have been extended to $r_0 = 1000$ jet diameters for acoustic sources and dipoles at angles $\Theta = 0^o$ and $\Theta = 30^o$. The results are shown in figures 4. Also included for comparison are the errors calculated when the base surfaces are used. From figures 4 it is evident that the phase and amplitude errors do not drop appreciably as the computations are extended to the far-field. Omission of the base surfaces may be

permissible if a five percent error is acceptable, or for preliminary studies. But, it is apparent that some other form of modeling is necessary for the base of the cylindrical Kirchhoff surface. Hopefully, the CFD solution can be extended to an area where there are few nonlinearities in the flow. Then, the base surface effects can be calculated directly. If this cannot be done, some other form of modeling will be necessary. The frequency domain formulation may hold some promise for this modeling. The current project will determine what, if anything, is needed in this regard.

The Kirchhoff method has also been used in preliminary jet acoustics calculations. The LES code discussed in section 5 was used to find the pressure and pressure derivatives due to a Mach 1.5 jet in a stagnant medium. The Kirchhoff surface was a cylinder with no bases extending 50 jet diameters downstream. The radius of the cylinder varied from one to five jet diameters. The Jet was excited at a frequency such that the Strouhal number, $\omega L/U$, was 0.125. 150 points were used along the length of the surface, and 256 temporal points per period of excitation were used. The results of the calculations are shown in figures 5. Figure 5a shows the variance of the RMS pressure amplitude with distance for an emission angle of 60^o measured from the x axis. Also shown is line denoting a $1/r_0$ relationship. It can be seen that the amplitudes follow the $1/r_0$ relationship fairly closely. The effects of grid stretching in the CFD calculation can be seen in the plot for $r_k = 5$ diameters. Here the pressure and derivatives are not as accurate which leads to the disagreement with the predictions due to $r_k = 2, 3, 4$. When r_k is equal to one diameter the surface does not enclose enough of the noise producing portions of the flow. Thus, a Kirchhoff surface of radius from two to four jet diameters is desirable for the acoustics calculations.

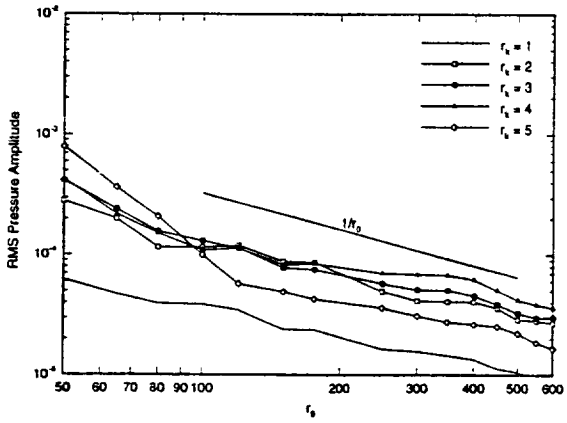

Figure 5a. RMS Pressure Amplitude with distance at $\Theta = 60^o$. $M_\infty = 1.5$ Jet.

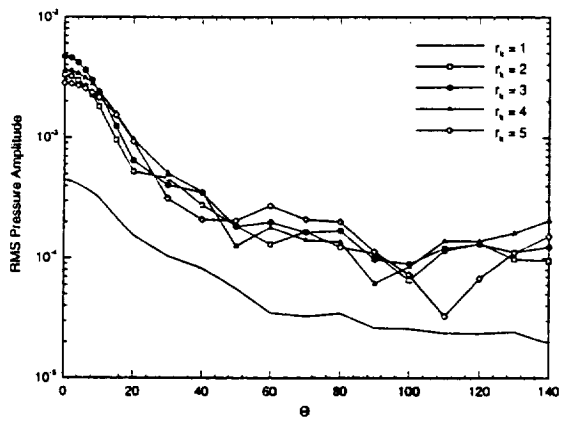

Figure 5b. RMS Pressure Amplitude with angle at $r_0 = 75.0$. $M_\infty = 1.5$ Jet.

Figure 5b shows the variance of the RMS pressure amplitude with emission angle for a distance of 75 jet diameters. The emitted sound is located mainly within 30^o of the jet axis. This is as expected. Again, the acceptable data is obtained with a Kirchhoff surface of radius two to four jet diameters.

7. Proposed Investigations

Upon the completion of preliminary investigations to determine errors and the validity of the Kirchhoff method. several proposed investigations will be undertaken. The main

focus of these investigations will be to determine dominant frequencies and intensities of different types of supersonic jet noise. Additionally, factors such as directivity and noise production mechanisms will be investigated. If possible, noise reduction techniques will be identified.

Initially, the Kirchhoff method is being be used to calculate the noise produced by perfectly expanded, axisymmetric jets. This study will be used to determine the effect of the LES turbulence modeling and the placement of the control surface. Results obtained through the use of the Kirchhoff method will be compared with those obtained by others through the use of experiments, acoustic analogy, and computations of the linearized Euler equations. Favorable comparisons are expected.

Predictions of imperfectly expanded jets will begin after the initial calculations are completed. The researcher will be investigating primarily the noise associated with shock waves in the jet flow. Screech tones can cause structural damage to aircraft, so this area of research is quite important. Additionally, the production of noise in shock wave–turbulence interactions and shock–vortex interactions will be investigated. These calculations will be performed with a fully three dimensional prediction method. Three dimensional directivity in supersonic jets has not yet been adequately investigated.

8. Conclusions

The Kirchhoff method is a powerful tool for aeroacoustics research. When used in conjunction with accurate CFD codes it allows for efficient, accurate calculation of far–field acoustic signatures. Nonlinearities and three dimensional effects are easily handled by the method. These properties make the Kirchhoff method an ideal choice for the study of supersonic jets. Excellent predictions are expected for a wide range of aeroacoustics problems.

9. Acknowledgments

This work is sponsored be NASA Langley Research Center under research grant no. NAG 1-1605 The technical monitor is Kristine Meadows. We are grateful for their assistance.

The LES code discussed in section 5 was provided by Reda Mankbadi of NASA Lewis Research Center.

10. References

[1] Tam, C.K.W., "Jet Noise Generated by Large Scale Coherent Motion," Chapter 6 in NASA RP–1258, 1991

[2] Kirchhoff, G.B., *Berliner Sitzungsber*, Vol. 641, 1882

[3] Lighthill, M.J., "On Sound Generated Aerodynamically, Part I, General Theory," *Proceedings of the Royal Society of London, Series A: Mathematical and Physical Sciences*, Vol. 211, Feb. 7 - March 20, 1952, pp. 564–587

[4] Neise, W, and Michel, U., "Aerodynamic Noise of Turbomachines," Deutsch Forschungsanstalt fur Luft– und Faumfahrt, e.V. DLR, Institut fur Stromungsmechanik, Abt. Turbulensforschung, Muller–Breslau–Str. 8, 10623 Berlin, Germany, Nov 25, 1994

[5] Lilley, G.M., " On the Noise From Jets: Noise Mechanisms," AGARD-CP-131, March 1974, 13.1-13.12

[6] Mankbadi, R.R., and Liu, J.T.C., "Sound Generated Aerodynamically Revisited: Large Scale Structures in a Turbulent Jet as a Source of Sound," *Philosophical Transactions of the Royal Society of London, Series A: Mathematical and Physical Sciences*, Vol. 311, No. 183, 1984, pp 183-217

[7] Mankbadi, R.R., Hayer, M.E., and Povinelli, L.A., "Structure of Supersonic Jet Flow and Its Radiated Sound," *AIAA Journal*, Vol. 32, No. 5, May 1994, pp 897-906

[8] Ffowcs Williams, J.E. and Hawkings, D.L., "Sound Generation by Turbulence and Surfaces in Arbitrary Motion," *Philosophical Transactions of the Royal Society of London*, Vol. 264A, 1969, pp. 321-342

[9] Tam, C.K.W., and Webb, J.C., "Dispersion-Relation-Preserving Schemes for Computational Acoustics," *Journal of Computational Physics*, Vol. 107, No. 2, 1993, pp 262-281

[10] Thomas, J.P., and Roe, P.L., "Development of Non-Dissipative Numerical Schemes for Computational Aeroacoustics," AIAA Paper No. 93-3382, June 1993

[11] Stoker, R.W., and Smith, M.J., "An Evaluation of Finite Volume Direct Simulation and Perturbation Methods in CAA Applications," AIAA Paper No. 93-0152, Jan. 1993.

[12] Mankbadi, R.R., "On the Use of Linearized Euler Equations in the Prediction of Jet Noise," AIAA Paper No. 95-0505, Jan. 1995

[13] Lyrintzis, A.S., and George, A.R., "Far-Field Noise of Transonic Blade-Vortex Interactions," *American Helicopter Society Journal*, Vol. 34, No. 3, 1989, pp. 30-39

[14] Lyrintzis, A.S., "Review: The Use of Kirchhoff's Method in Computational Aeroacoustics," *ASME Journal of Fluids Engineering*, Vol. 116, Dec. 1994, pp. 665-676

[15] Morino, L., "Mathematical Foundations of Integral Methods," in *Computational Methods in Potential Aerodynamics*, Editor L. Morino, Springer-Verlag, New York, 1985, pp. 271-291

[16] Davis, C.M., and Atassi, H.M., "The Far-Field Acoustic Pressure of an Airfoil in Nonuniform Subsonic Flows," presented at the symposium on *Flow Noise Modeling, Measurement and Control*, NCA-Vol. 11/FED-Vol. 130, pp. 107-117, ASME Winter Annual Meeting, Atlanta, GA, Dec. 1991

[17] Smagorinski, J., "General Circulation Experiments with the Primitive Equations. I. The Basic Experiment," *Monthly Weather Review*, Vol. 91, 1963, pp 99-164

[18] Lyrintzis, A.S., and Mankbadi, R.R., "On the Prediction of the Far-Field Jet Noise Using Kirchhoff's Formulation," AIAA Paper No. 95-0508, Jan. 1995

[19] Yee, H.C., "A Class of High Resolution Explicit and Implicit Shock Capturing Schemes," NASA TM-101088, February 1989

[20] Harten, A. and Osher, S., "Uniformly High Order Accurate Nonoscillatory Schemes I," SIAM J. Numer. Anal., Vol. 24, No. 2, April 1987, pp. 279-309

[21] Atkins, H.L., "High-Order ENO Methods for the Unsteady Compressible Navier-Stokes Equations," AIAA Paper No. 91-1557, June 1991

[22] Shu, C.W., "Total-Variation-Diminishing Time Discretizations," *SIAM Journal of Scientific Computation*, Vol. 9, No. 6, 1988, pp 1073-1084

[23] Casper, J. and Meadows, K.R., "Using High Order Essentially Non-Oscillatory Schemes for Aeroacoustic Applications," AIAA Paper No. 95-0163, Jan. 1995

[24] Atkins, H. and Casper, J., "Nonreflective Boundary Conditions for High-Order Methods," *AIAA Journal*, Vol. 32, No. 3, March 1994, pp 512-518

11. Appendix

The method to advance U at time level n to level $n+2$ with the 2-4 MacCormack method is shown below.

$$U_{i,j}^{n+\frac{1}{2}} = U_{i,j}^{n} + \frac{\Delta t}{6\Delta r}\Big[7\Big(G_{i,j+1} - G_{i,j}\Big) - \Big(G_{i,j+2} - G_{i,j+1}\Big)\Big]^{n} + \Delta t W_{i,j}^{n} \tag{11.1}$$

$$U_{i,j}^{n+1} = \frac{1}{2}\Bigg\{U_{i,j}^{n+\frac{1}{2}} + U_{i,j}^{n} + \frac{\Delta t}{6\Delta r}\Big[7\Big(G_{i,j} - G_{i,j-1}\Big) - \Big(G_{i,j-1} - G_{i,j-2}\Big)\Big]^{n+\frac{1}{2}} + \Delta t W_{i,j}^{n+\frac{1}{2}}\Bigg\} \tag{11.2}$$

$$U_{i,j}^{n+\frac{3}{2}} = U_{i,j}^{n+1} + \frac{\Delta t}{6\Delta r}\Big[7\Big(G_{i,j} - G_{i,j-1}\Big) - \Big(G_{i,j-1} - G_{i,j-2}\Big)\Big]^{n+1} + \Delta t W_{i,j}^{n+1} \tag{11.3}$$

$$U_{i,j}^{n+2} = \frac{1}{2}\Bigg\{U_{i,j}^{n+1} + U_{i,j}^{n+\frac{3}{2}} + \frac{\Delta t}{6\Delta r}\Big[7\Big(G_{i,j+1} - G_{i,j}\Big) - \Big(G_{i,j+2} - G_{i,j+1}\Big)\Big]^{n+\frac{3}{2}} + \Delta t W_{i,j}^{n+\frac{3}{2}}\Bigg\} \tag{11.4}$$

and

$$U_{i,j}^{n+\frac{1}{2}} = U_{i,j}^{n} + \frac{\Delta t}{6\Delta x}\Big[7\Big(F_{i+1,j} - F_{i,j}\Big) - \Big(F_{i+2,j} - F_{i+1,j}\Big)\Big]^{n} \tag{11.5}$$

$$U_{i,j}^{n+1} = \frac{1}{2}\Bigg\{U_{i,j}^{n+\frac{1}{2}} + U_{i,j}^{n} + \frac{\Delta t}{6\Delta x}\Big[7\Big(F_{i,j} - F_{i-1,j}\Big) - \Big(F_{i-1,j} - F_{i-2,j}\Big)\Big]^{n+\frac{1}{2}}\Bigg\} \tag{11.6}$$

$$U_{i,j}^{n+\frac{3}{2}} = U_{i,j}^{n+1} + \frac{\Delta t}{6\Delta x}\Big[7\Big(F_{i,j} - F_{i-1,j}\Big) - \Big(F_{i-1,j} - F_{i-2,j}\Big)\Big]^{n+1} \tag{11.7}$$

$$U_{i,j}^{n+2} = \frac{1}{2}\Bigg\{U_{i,j}^{n+1} + U_{i,j}^{n+\frac{3}{2}} + \frac{\Delta t}{6\Delta x}\Big[7\Big(F_{i+1,j} - F_{i,j}\Big) - \Big(F_{i+2,j} - F_{i+1,j}\Big)\Big]^{n+\frac{3}{2}}\Bigg\} \tag{11.8}$$